A Tungsten Silyl Alkylidyne Complex and Its Bis(alkylidene) Tautomer. Their Interconversion and an Unusual Silyl Migration in Their Reaction with Dioxygen

Tianniu Chen,[†] Xin-Hao Zhang,[‡] Changsheng Wang,[‡,#] Shujian Chen,[†] Zhongzhi Wu,[†] Liting Li,[†] Karn R. Sorasaenee,[†] Jonathan B. Diminnie,[†] Hongjun Pan,[†] Ilia A. Guzei,[§,⊥] Arnold L. Rheingold,[§,∥] Yun-Dong Wu,*[,‡] and Zi-Ling Xue*[,†]

Department of Chemistry, The University of Tennessee, Knoxville, Tennessee 37996-1600, Department of Chemistry, The Hong Kong University of Science and Technology, Clear Water Bay, Hong Kong, China, and Department of Chemistry & Biochemistry, The University of Delaware, Newark, Delaware 19716-2522

Received December 8, 2004

Bis(alkylidene) complex W(=CH-*t*-Bu)$_2$(CH$_2$-*t*-Bu)(Si-*t*-BuPh$_2$) (**1a**) has been found to be in equilibrium with its alkyl alkylidyne tautomer W(≡C-*t*-Bu)(CH$_2$-*t*-Bu)$_2$(Si-*t*-BuPh$_2$) (**1b**). Bis(alkylidene) complexes are believed to be intermediates in α-H transfer in alkylidyne complexes W(≡CSiMe$_3$)(CH$_2$-*t*-Bu)$_3$ and W(≡^{13}C-*t*-Bu)(CH$_2$-*t*-Bu)$_3$. The current study represents a rare observation of an exchange between a bis(alkylidene) and an alkyl alkylidyne complex. Thermodynamics and kinetics of the exchange **1a** ⇌ **1b** have been studied. The equilibrium constant K_{eq} for the exchange **1a** ⇌ **1b** is 3.34(0.05) at 287(1) K, and the thermodynamic parameters of the equilibrium measured are $\Delta H° = -3.8(0.8)$ kJ/mol, $\Delta S° = -3(3)$ J/mol·K, and $\Delta G°_{287K} = -3(2)$ kJ/mol. The rate constants k_1 and k_{-1} were obtained from 2D exchange spectroscopy between 267 and 297 K and are 0.34(0.03) and 0.10(0.01) s^{-1}, respectively, at 287 K. For the conversion **1a** → **1b**, activation enthalpy and entropy are $\Delta H^‡_1 = 75(5)$ kJ/mol, $\Delta S^‡_1 = 8(25)$ J/mol·K; for the conversion **1b** → **1a**, $\Delta H^‡_{-1} = 78(5)$ kJ/mol, $\Delta S^‡_{-1} = 8(25)$ J/mol·K. In the reaction of **1** with O$_2$, the silyl ligand in **1b** was found to undergo an unprecedented migration to the alkylidyne ligand to give the alkylidene oxo complex W(=O)[=C(*t*-Bu)(Si-*t*-BuPh$_2$)](CH$_2$-*t*-Bu)$_2$ (**2**). The structure of **2** has been determined. Density functional theory calculations have been conducted for a series of model 1,2-migration reactions. The results suggest that the formation of **2** might be initiated by a 1,2-silyl migration to generate a triplet W-alkylidene intermediate, which is then trapped by O$_2$.

Introduction

Transition metal silyl complexes have shown unique chemistry different from their alkyl analogues.[1] We have been interested in d^0 silyl alkylidyne complexes M(≡CR)(CH$_2$R)$_2$SiR′$_3$ [R′$_3$ = Ph$_2$-*t*-Bu, **1b**; (SiMe$_3$)$_3$, **3**; R = *t*-Bu] in part because there are few such complexes and their chemistry is largely unknown. The reactivity of α-H atoms in such alkyl alkylidyne complexes has been the subject of many studies, as these hydrogen atoms often play a pivotal role in the formation of the high-oxidation-state complexes.[2,3] The α-H atoms in d^0

* To whom correspondence should be addressed. E-mail: xue@utk.edu; chydwu@ust.hk.
† The University of Tennessee.
‡ The Hong Kong University of Science and Technology.
# Current address: Department of Chemistry, Liaoning Normal University, Dalian 116029, China.
§ The University of Delaware.
⊥ Current address: Department of Chemistry, The University of Wisconsin−Madison, Madison, WI 53706-1396.
∥ Current address: Department of Chemistry and Biochemistry, University of California−San Diego, La Jolla, CA 92093-0332.

(1) (a) Tilley, T. D. In *The Silicon-Heteroatom Bond*; Patai, S., Rappoport, Z., Eds.; Wiley: New York, 1991; p 245 and p 309. (b) Eisen, M. S. In *The Chemistry of Organic Silicon Compounds*, Vol. 2, Rappoport, Z., Apeloig, Y., Eds.; Wiley: New York, 1998, Part 3, p 2037. (c) Corey, J. Y.; Braddock-Wilking, J. *Chem. Rev.* **1999**, *99*, 175. (d) Sharma, H. K.; Pannell, K. H. *Chem. Rev.* **1995**, *95*, 1351. (e) Harrod, J. F.; Mu, Y.; Samuel, E. *Polyhedron* **1991**, *10*, 1239. (f) Reichl, J. A.; Berry, D. H. *Adv. Organomet. Chem.* **1998**, *43*, 197. (g) Yu, X.-H.; Morton, L. A.; Xue, Z.-L. *Organometallics* **2004**, *23*, 2210.

(2) (a) Schrock, R. R. *Chem. Rev.* **2002,** *102*, 145. (b) Schrock, R. R. *Dalton Trans.* **2001**, 2541. (c) Feldman, J.; Schrock, R. R. *Prog. Inorg. Chem.* **1991**, *39*, 1. (d) Aguero, A.; Osborn, J. A. *New J. Chem.* **1988**, *12*, 111. (e) Mayr, A.; Hoffmeister, H. *Adv. Organomet. Chem.* **1991**, *32*, 227. (f) Schubert, U. In *Carbyne Complexes*; VCH: New York, 1988; p 39. (g) Nugent, W. A.; Mayer, J. M. *Metal−Ligand Multiple Bonds*; Wiley: New York, 1988. (h) Kim, H. P.; Angelici, R. J. *Adv. Organomet. Chem.* **1987**, *27*, 51. (i) Schrock, R. R.; Fellmann, J. D. *J. Am. Chem. Soc.* **1978**, *100*, 3359. (j) Clark, D. N.; Schrock, R. R. *J. Am. Chem. Soc.* **1978**, *100*, 6774. (k) Mowat, W.; Wilkinson, G. *J. Chem. Soc., Dalton Trans.* **1973**, 1120. (l) Andersen, R. A.; Chisholm, M. H.; Gibson, J. F.; Reichert, W. W.; Rothwell, I. P.; Wilkinson, G. *Inorg. Chem.* **1981**, *20*, 3934. (m) Li, L.; Hung, M.; Xue, Z. *J. Am. Chem. Soc.* **1995**, *117*, 12746. (n) Xue, Z.; Li, L.; Hoyt, L. K.; Diminnie, J. B.; Pollitte, J. L. *J. Am. Chem. Soc.* **1994**, *116*, 2169. (o) Li, L.-T.; Diminnie, J. B.; Liu, X.-Z.; Pollitte, J. L.; Xue, Z.-L. *Organometallics* **1996**, *15*, 3520.

(3) For d^n type carbenes and carbynes, see, e.g., refs 2e−h and: (a) Trnka, T. M.; Grubbs, R. H. *Acc. Chem. Res.* **2001**, *34*, 18. (b) Schrock, R. R.; Hoveyda, A. H. *Angew. Chem., Int. Ed.* **2003**, *42*, 4592. (c) Pollagi, T. P.; Manna, J.; Stoner, T. C.; Geib, S. J.; Hopkins, M. D. *NATO ASI Series C* **1993**, *392*, 71. (d) Yong, B. S.; Nolan, S. P. *Chemtracts* **2003**, *16*, 205. (e) Doyle, M. P. *Pure Appl. Chem.* **1998**, *70*, 1123.

10.1021/om049031j CCC: $30.25
Publication on Web 02/17/2005

alkyl alkylidyne complexes W(≡CR′)(CH_2R)$_3$ are also known to undergo exchanges among the α-C atoms, leading to alkyl−alkylidyne scrambling in W(≡^{13}C-*t*-Bu)(CH_2-*t*-Bu)$_3$ and W(≡CSiMe$_3$)(CH_2-*t*-Bu)$_3$ (eqs 1, 2).[4] Deuterium-labeling and kinetic studies of the α-H migration in W(≡CSiMe$_3$)(CH_2-*t*-Bu)$_3$ showed stepwise transfer of two H atoms in one alkyl ligand to the alkylidyne ligand with the proposed bis(alkylidene) intermediate "W(=CHSiMe$_3$)(=CH-*t*-Bu)(CH_2-*t*-Bu)$_2$" (eq 1).[4b] H/D scrambling was also observed in the d^2 Os bis(alkylidene) complex Os(=CH-*t*-Bu)$_2$(CD_2-*t*-Bu)$_2$, and this exchange is believed to involve the alkylidyne intermediate "Os(≡C-*t*-Bu)(CD_2-*t*-Bu)$_2$(CH_2-*t*-Bu)" (eq 3).[5]

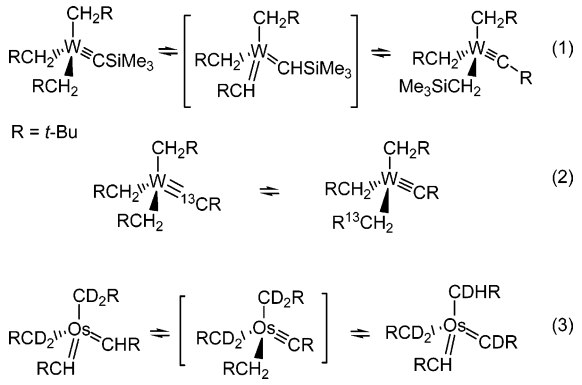

High-oxidation-state bis(alkylidene) complexes were first reported by Schrock, Churchill, and co-workers.[6] Direct observations of exchanges between alkyl alkylidyne and bis(alkylidene) tautomers are rare.[7] The phosphine-promoted exchange W(≡CSiMe$_3$)(CH_2SiMe_3)$_3$(PMe$_3$) ⇌ W(=CHSiMe$_3$)$_2$(CH_2SiMe_3)$_2$(PMe$_3$) was recently reported.[7] In the absence of phosphine, bis(alkylidene) "W(=CHSiMe$_3$)$_2$(CH_2SiMe_3)$_2$" was not observed. d^0-Silyl alkylidyne complex W(≡C-*t*-Bu)(CH_2-*t*-Bu)$_2$(Si-*t*-BuPh$_2$) (**1b**) has been found to exchange with its bis(alkylidene) tautomer W(=CH-*t*-Bu)$_2$(CH_2-*t*-Bu)(Si-*t*-BuPh$_2$) (**1a**).[8] The silyl ligand in **1a/1b** clearly plays an important role in the current alkyl alkylidyne−bis(alkylidene) exchange, as no such exchange has been directly observed in W(≡^{13}C-*t*-Bu)(CH_2-*t*-Bu)$_3$, the alkyl analogue of **1b** (eq 2).[4a]

We were also surprised to find that the equilibrium mixture of d^0 **1a** ⇌ **1b** reacts with O_2 to give a silyl-substituted alkylidene oxo complex, W(=O)[=C(*t*-Bu)(Si-*t*-BuPh$_2$)](CH_2-*t*-Bu)$_2$ (**2**). In this reaction, the silyl ligand in d^0 W(≡C-*t*-Bu)(CH_2-*t*-Bu)$_2$(Si-*t*-BuPh$_2$) (**1b**) undergoes an unprecedented migration to the alkylidyne ligand in **1b** to give the alkylidene ligand in **2**. In comparison, we found that W(≡C-*t*-Bu)(CH_2-*t*-Bu)$_2$[Si(SiMe$_3$)$_3$] (**3**),[2n] which differs from **1b** only in the silyl group, reacts with O_2 to give HSi(SiMe$_3$)$_3$ and other unidentified decomposition products.

Although reactions of O_2 with metal complexes are of fundamental importance to many catalytic and biological processes, studies of such reactions have been mostly concentrated to d^n complexes.[9,10] Oxidation of the metals is often involved in these reactions with O_2. Although many d^0 early transition metal complexes are O_2-sentitive, the nature of the reactions of these complexes with O_2 is largely unknown. Few studies have been conducted of the reactions of O_2 with d^0 high-oxidation-state transition metal complexes. Schwartz,[10a] Gibson,[10b] and co-workers reported oxygen insertion into the Zr−R bond in the reaction of $ZrCp_2RCl$ with O_2. Similar reactions between $ZrCp_2R_2$ and O_2 were shown by Brindley and Scotton to give $ZrCp_2(OR)_2$.[10c] Bercaw and co-workers studied the conversion of $HfCp^*_2(R)$(OO-*t*-Bu) to $HfCp^*_2$(OR)(O-*t*-Bu).[10d] In Cp-free complexes, Wolczanski, Rothwell, Gibson, and their co-workers reported reactions of O_2 with Ti(OR)$_2$Me$_2$,[10e] Ta(OAr)$_2$Me$_3$,[10f] and Mo(=NAr)$_2$Me$_2$[10g] to yield Ti(OR)$_2$(OMe)$_2$,

(4) (a) Xue, Z.; Chuang, S.-H.; Caulton, K. G.; Chisholm, M. H. *Chem. Mater.* **1998**, *10*, 2365. (b) Caulton, K. G.; Chisholm, M. H.; Streib, W. E.; Xue, Z. *J. Am. Chem. Soc.* **1991**, *113*, 6082. (c) Xue, Z.; Caulton, K. G.; Chisholm, M. H. *Chem. Mater.* **1991**, *3*, 384.

(5) (a) LaPointe, A. M.; Schrock, R. R.; Davis, W. M. *J. Am. Chem. Soc.* **1995**, *117*, 4802. (b) LaPointe, A. M.; Schrock, R. R. *Organometallics* **1995**, *14*, 1875.

(6) (a) Fellmann, J. D.; Rupprecht, G. A.; Wood, C. D.; Schrock, R. R. *J. Am. Chem. Soc.* **1978**, *100*, 5964. (b) Churchill, M. R.; Youngs, W. J. *Inorg. Chem.* **1979**, *18*, 1930. (c) Fellmann, J. D.; Schrock, R. R.; Rupprecht, G. A. *J. Am. Chem. Soc.* **1981**, *103*, 5752. See also: (d) Diminnie, J. B.; Hall, H. D.; Xue, Z.-L. *Chem. Commun.* **1996**, 2383. (e) Diminnie, J. B.; Blanton, J. R.; Cai, H.; Quisenberry, K. T.; Xue, Z. *Organometallics* **2001**, *20*, 1504.

(7) Morton, L. A. Zhang, X.-H.; Wang, R.; Lin, Z.; Wu, Y.-D.; Xue, Z.-L. *J. Am. Chem. Soc.* **2004**, *33*, 10208.

(8) Preliminary results were published earlier. Chen, T.-N.; Wu, Z.-Z.; Li, L.-T.; Sorasaenee, K. R.; Diminnie, J. B.; Pan, H.-J.; Guzei, I. A.; Rheingold, A. L.; Xue, Z.-L. *J. Am. Chem. Soc.* **1998**, *120*, 13519.

(9) (a) Sheldon, R. A.; Kochi, J. K. *Metal Catalyzed Oxidations of Organic Compounds*; Academic Press: New York, 1981. (b) *The Activation of Dioxygen and Homogeneous Catalytic Oxidation*; Barton, D. H., Martell, A. E., Sawyer, D. T., Eds.; Plenum: Press: New York, 1993. *Oxygen Complexes and Activation by Transition Metals*, Martell, A. E., Sawyer, D. T., Eds.; Plenum Press: New York, 1988. (c) *Chem. Rev.* **1994**, *94*, Issue 3 (Klotz, I. M., Kurtz, D. M., Jr., Eds.). All papers in this issue on metal-dioxygen complexes. (d) Holm, R. H. *Chem. Rev.* **1987**, *87*, 1401. (e) Mirica, L. M.; Ottenwaelder, X.; Stack, T. D. P. *Chem. Rev.* **2004**, *104*, 1013. (f) Lewis, E. A.; Tolman, W. B. *Chem. Rev.* **2004**, *104*, 1047. (g) Baldwin, M. J. *Chemtracts* **2003**, *16*, 701. (h) Espenson, J. H. *Adv. Inorg. Chem.* **2003**, *54*, 157. (i) Roesky, H. W.; Haiduc, I.; Hosmane, N. S. *Chem. Rev.* **2003**, *103*, 2579. (j) Zhang, C. X.; Liang, H.-C.; Humphreys, K. J.; Karlin, K. D. *Catal. Met. Complexes* **2003**, *26*, 79. (k) Theopold, K. H.; Reinaud, O. M.; Blanchard, S.; Leelasubcharoen, S.; Hess, A.; Thyagarajan, S. *ACS Symp. Ser.* **2002**, *823*, 75. (l) Tolman, W. B.; Que, L., Jr. *J. Chem. Soc., Dalton Trans.* **2002**, *5*, 653. (m) Blackman, A. G.; Tolman, W. B. *Struct. Bonding (Berlin)* **2000**, *97*, 179. (n) Zuberbuhler, A. *Chimia* **1999**, *53*, 239. (o) Suzuki, M. *Pure Appl. Chem.* **1998**, *70*, 955. (p) Bianchini, C.; Zoellner, R. W. *Adv. Inorg. Chem.* **1997**, *44*, 263. (q) Bakac, A. *Prog. Inorg. Chem.* **1995**, *43*, 267.

(10) (a) Blackburn, T. F.; Labinger, J. A.; Schwartz, J. *Tetrahedron Lett.* **1975**, *16*, 3041. Labinger, J. A.; Hart, D. W.; Seibert, W. E.; Schwartz, J. *J. Am. Chem. Soc.* **1975**, *97*, 3851. (b) Gibson, T. *Organometallics* **1987**, *6*, 918. (c) Brindley, P. B.; Scotton, M. J. *J. Chem. Soc., Perkin Trans. 2* **1981**, 419. (d) Van Asselt, A.; Santarsiero, B. D.; Bercaw, J. E. *J. Am. Chem. Soc.* **1986**, *108*, 8291. Coughlin, E. B.; Bercaw, J. E. *Organometallics* **1992**, *11*, 465. (e) Lubben, T. V.; Wolczanski, P. T. *J. Am. Chem. Soc.* **1987**, *109*, 424. Lubben, T. V.; Wolczanski, P. T. *J. Am. Chem. Soc.* **1985**, *107*, 701. (f) Wang, R.-J.; Folting, K.; Huffman, J. C.; Chamberlain, L. R.; Rothwell, I. P. *Inorg. Chim. Acta* **1986**, *120*, 81. (g) Gibson, V. C.; Redshaw, C.; Walker, G. L. P.; Howard, J. A. K.; Hoy, V. J.; Cole, J. M.; Kuzmina, L. G.; De Silva, D. S. *J. Chem. Soc., Dalton Trans.* **1999**, 161. (h) Brindley, P. B.; Hodgson, J. C. *J. Organomet. Chem.* **1974**, *65*, 57. (i) Kim, S.-J.; Jung, I. N.; Yoo, B. R.; Cho, S.; Ko, J.; Kim, S. H.; Kang, S. O. *Organometallics* **2001**, *20*, 1501. (j) Schaverien, C. J.; Orpen, A. G. *Inorg. Chem.* **1991**, *30*, 4968. Schaverien, C. J. *J. Chem. Soc., Chem. Commun.* **1991**, 458. (k) Adam and co-workers used O_2 to oxidize d^0 Ti enolates to give α-hydroxy amides. Adam, W.; Metz, M.; Prechtl, F.; Renz, M. *Synthesis* **1994**, 563. (l) Adam and co-workers used oxidation of alkenyl complexes Tp*W(=O)$_2$R by singlet $^1O_2$ to yield allylic hydroperoxides. Adam, W.; Putterlik, J.; Schuhmann, R. M.; Sundermeyer, J. *Organometallics* **1996**, *15*, 4586. (m) In the reaction of $L_2Mo(=O)(CH_2R)_2$ (L = 4,4′-dimethyl-2,2′-dipyridyl) with $^{18}O_2$, Sen and Vetter observed the formation of RCH=^{18}O and decomposition of the complex. Vetter, W. M.; Sen, A. *Organometallics* **1991**, *10*, 244. (n) Bercaw and co-workers found that the formation of $Cp^*_2Ta(CH_2R)(\eta^2\text{-}O_2)$ [and later $Cp^*_2Ta(O{-}CH_2R)(=O)$] in the reaction of d^0 $Cp^*_2Ta(=CHR)H$ with O_2 is consistent with a mechanism involving a d^2 intermediate "$Cp^*_2Ta(CH_2R)$". van Asselt, A.; Trimmer, M. S.; Henling, L. M.; Bercaw, J. E. *J. Am. Chem. Soc.* **1988**, *110*, 8254.

Scheme 1. Preparation of d⁰ W Silyl Alkylidyne Complex 1b and Its Exchange with the Bis(alkylidene) Tautomer 1a

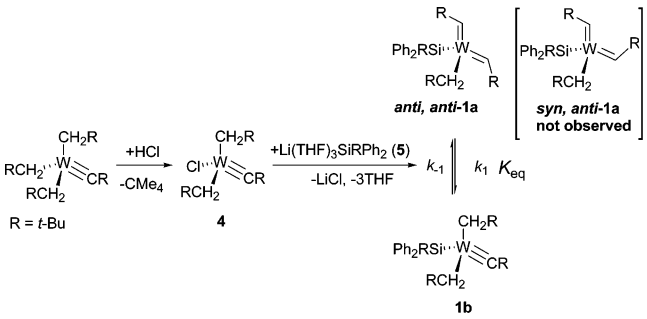

$Ta(OAr)_2(OMe)_3$, and $[Mo(=NAr)_2Me(\mu\text{-}OMe)]_2$, respectively (eq 4). Autoxidation of $M(CH_2R)_4$ by O_2 was found to be rapid.[10h] Yoo and co-workers found that reactions of O_2 with chelating diamides Ti(N∼N)MeX (X = Me, Cl; N∼N = silacyclo-alkane or -alkene bridge) gave $[Ti(N\sim N)(\mu\text{-}OMe)X]_2$.[10i] In contrast, the reaction of alkyl-free $Ti(N\sim N)Cl_2$ with O_2 led to diamide ligand oxidation.[10i] Schaverien and Orpen reported that $AlLY(\mu\text{-}Me)_2Me_2$ (L = porphyrin) activates O_2 to give $AlLY(\mu\text{-}OMe)_2Me_2$.[10j]

$$MR_n \xrightarrow{n/2\ O_2} M(OR)_n \qquad (4)$$

We have investigated thermodynamics and kinetics of the unusual bis(alkylidene) ⇌ alkyl alkylidyne exchange W(=CH-*t*-Bu)$_2$(CH$_2$-*t*-Bu)(Si-*t*-BuPh$_2$) (**1a**) ⇌ W(≡C-*t*-Bu)(CH$_2$-*t*-Bu)$_2$(Si-*t*-BuPh$_2$) (**1b**). Experimental and theoretical studies have also been conducted to explore the mechanistic pathways in the formation of the silyl-substituted alkylidene oxo complex W(=O)-[=C(*t*-Bu)(Si-*t*-BuPh$_2$)](CH$_2$-*t*-Bu)$_2$ (**2**). Theoretical studies have been performed to model the silyl migration in **1b** to give **2** and potential silyl migration in **3**. These studies and the preparation and characterization of **1** and **2** are reported.

Results and Discussion

Preparation and Characterization of d⁰ W Silyl Alkylidyne Complex 1b. The addition of 1 equiv of HCl to W(≡C-*t*-Bu)(CH$_2$-*t*-Bu)$_3$[11] led to the formation of thermally unstable alkylidyne W(≡C-*t*-Bu)(CH$_2$-*t*-Bu)$_2$-Cl (**4**). The reaction of **4** with 1 equiv of Li(THF)$_3$Si-*t*-BuPh$_2$ (**5**)[12] at −40 °C (Scheme 1), followed by workup of the product at −10 °C and crystallization at −30 °C, yielded crystalline **1** in 58% yield (Scheme 1). Spectroscopic properties [^{1}H, ^{13}C{^{1}H}, ^{1}H-gated-decoupled ^{13}C, ^{1}H−^{13}C heteronuclear correlation (HETCOR), and ^{29}Si-{^{1}H} NMR] of **1a** and **1b** were consistent with the structure assignments and the existence of the two tautomers in solution. The resonances of the alkylidene ligands in **1a** and alkylidyne ligand in **1b** appeared as a doublet at 272.30 ppm and a singlet at 318.38 ppm, respectively, in the ^{1}H-gated-decoupled ^{13}C spectra. There was one ^{1}H NMR resonance at 6.03 ppm (=C*H*-*t*-Bu) for the two alkylidene ligands in **1a** between −20 and 20 °C. This observation suggests that the two alkylidene ligands adopt an *anti*,*anti*-configuration, and it is unlikely that these two ligands are involved in a fast rotation about the W=C bonds. Barriers to the rotation of alkylidene ligands about the M=C bonds are usually high.[2a] The *anti*,*anti*-configuration has also been observed in Os(=CH-*t*-Bu)$_2$(CH$_2$-*t*-Bu)$_2$.[5a] The prochiral W atom in **1b** gives rise to diastereotopic methylene (C*H*$_a$*H*$_b$-*t*-Bu) protons with chemical shifts of 2.08 and −0.77 ppm ($^2J_{Ha-Hb}$ = 11.9 Hz). The mixture of **1a** and **1b** is stable as a solid, but slowly decomposes in solution at room temperature, forming HSi-*t*-BuPh$_2$ and unknown species.

Table 1. Equilibrium Constants (K_{Eq}) for 1a ⇌ 1b

T (K)	$K_{eq}[\sigma K_{eq(ran)}]$ [a]
287(1)	3.34(0.05)
282(1)	3.45(0.04)
277(1)	3.520(0.005)
272(1)	3.620(0.015)
267(1)	3.760(0.004)
262(1)	3.860(0.001)
257(1)	3.990(0.016)
252(1)	4.130(0.011)
247(1)	4.260(0.004)
242(1)	4.450(0.002)
237(1)	4.590(0.006)

[a] The largest random uncertainty is $\sigma K_{eq(ran)}/K_{eq}$ = 0.05/3.34 = 1.5%. The total uncertainty $\sigma K_{eq}/K_{eq}$ of 5.2% was calculated from $\sigma K_{eq(ran)}/K_{eq}$ = 1.5% and the estimated systematic uncertainty $\sigma K_{eq(sys)}/K_{eq}$ = 5% by $\sigma K_{eq}/K_{eq} = [(\sigma K_{eq(ran)}/K_{eq})^2 + (\sigma K_{eq(sys)}/K_{eq})^2]^{1/2}$.

In the solid-state CPMAS (cross-polarization magic angle spinning) ^{13}C{^{1}H} NMR spectrum of crystalline **1** at 23 °C, both **1a** and **1b** were observed, indicating that both isomers are present even in the crystalline solids.[13] Crystals of **1** were found to be severely disordered, and attempts to fully refine the structure of **1** were unsuccessful. The presence of both **1a** and **1b** as well as their α-H exchange in the solid state, as observed in the ^{13}C SSNMR of **1** (**1a**/**1b**),[13] may lead to the disorder in the structure of **1**.

In the 2D NOESY spectra of **1a** and **1b** at 296 K (t_{mix} = 3 s), strong *positive* cross-peaks were observed between the methylene (C*H*$_a$*H*$_b$-*t*-Bu) protons in **1b** and the alkylidene (=C*H*-*t*-Bu) and methylene (C*H*$_2$-*t*-Bu) protons in **1a**, consistent with a chemical exchange process between **1a** and **1b** at this temperature.

Thermodynamic Studies of the Exchange 1a ⇌ 1b. Variable-temperature NMR spectra of the isomerization bis(alkylidene) **1a** ⇌ alkylidyne **1b** were studied, and the equilibrium constants, K_{eq} = [**1b**]/[**1a**], measured between 237 and 287 K are listed in Table 1. A plot of ln K_{eq} vs 1/T (Figure 1) gave a linear fit and yielded $\Delta H°$ = −3.8(0.8) kJ/mol and $\Delta S°$ = −3(3) J/mol·K. The equilibrium constants K_{eq} range from 4.590(0.006) at 237 K to 3.34(0.05) at 287 K, indicating that the alkylidyne **1b** is favored, and increasing the temperature shifts the equilibrium toward bis(alkylidene) **1a**. The process **1a** ⇌ **1b** is slightly exothermic with $\Delta H°$ = −3.8(0.8) kJ/mol. This enthalpy change outweighs the entropy change [$\Delta S°$ = −3(3) J/mol·K] in the isomerization **1a** ⇌ **1b** to give $\Delta G°$ = −2.9(1.7) kJ/mol at 287(1) K in favor of **1b**. Increasing the temperature shifts the equilibrium toward the alkylidyne tautomer. In comparison, the bis(alkylidene) tautomer is favored in

(11) Schrock, R. R.; Sancho, J.; Pederson, S. F. *Inorg. Synth.* **1989**, *26*, 44.

(12) Campion, B. K.; Heyn, R. H.; Tilley, T. D. *Organometallics* **1993**, *12*, 2584.

(13) See Supporting Information for details.

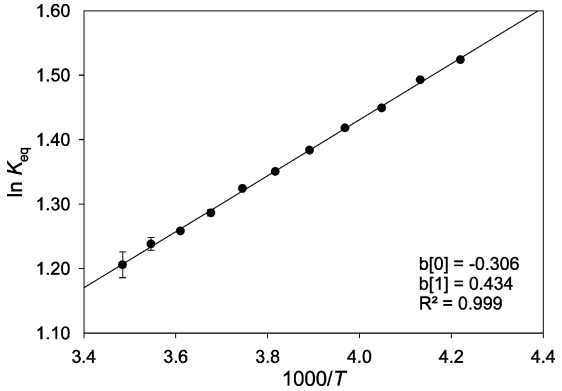

Figure 1. Plot of ln K_{eq} vs $1/T$ of the equilibrium **1a** ⇌ **1b**.

the other known, PMe_3-promoted alkylidyne ⇌ bis(alkylidene) exchange, $W(\equiv CSiMe_3)(CH_2SiMe_3)_3(PMe_3)$ ⇌ $W(=CHSiMe_3)_2(CH_2SiMe_3)_2(PMe_3)$. K_{eq} ranges from 9.37(0.12) at 303(1) K to 12.3(0.2) at 278(1) K, and $\Delta H° = -8(2)$ kJ/mol, $\Delta S° = -6(7)$ J/mol·K for this equilibrium.[7]

It is interesting to note that the d^0 alkylidyne complex **1b** is thermodynamically close in energy to its bis(alkylidene) isomer **1a**, although **1b** is slightly more stable. In the α-H exchange in $W(\equiv CSiMe_3)(CH_2\text{-}t\text{-}Bu)_3$ ⇌ $W(CH_2SiMe_3)(\equiv C\text{-}t\text{-}Bu)(CH_2\text{-}t\text{-}Bu)_2$, the proposed bis(alkylidene) intermediate "$W(=CHSiMe_3)(=CH\text{-}t\text{-}Bu)(CH_2\text{-}t\text{-}Bu)_2$" is so much higher in energy than the ground-state alkylidyne structure that this intermediate is not observed.[4]

Kinetic Studies of the Exchange 1a ⇌ 1b. 2D exchange spectroscopy (2D EXSY) based on the 2D NOESY pulse sequence has been established as a powerful structure determination method.[14−17] Quantitative exchange rates could also be derived from this 2D EXSY experiment with a careful choice of the mixing time lengths.[16] The kinetics of the exchange among α-H atoms in **1a** and **1b** was investigated between 267 and 297 K by 2D exchange spectroscopy. Representative phase-sensitive ^{1}H EXSY spectra of (**1a**/**1b**) are shown in the Supporting Information.[13] At temperatures ≤267 K, cross-peaks between C*H*= (**1a**)/CH_aH_b (**1b**) and between CH_2 (**1a**)/CH_aH_b (**1b**) were too weak to be detected,[13] indicating that the exchange was nearly frozen at these temperatures. As the temperature was increased, the intensities of the exchange cross-peaks increased. Between 277 and 297 K, the spectra[13] displayed high-intensity cross-peaks for C*H*= (**1a**)/CH_aH_b (**1b**) and for CH_2 (**1a**)/CH_aH_b (**1b**), respectively, as expected for the exchange process. The 2D EXSY data were treated quantitatively using the methods summarized by Perrin and Dwyer.[16] Each of the sets of diagonal and cross-peak intensities was processed, assuming a two-site exchange system according to eqs 5 and 6, in which k' is the sum of the forward and reverse rate constants, t_m is the mixing time, X denotes the mole fractions of the two sites, which is a variable and calculated from K_{eq} in the aforementioned variable-temperature 1D NMR, I_{1a1a} and I_{1b1b} are the diagonal peak intensities of **1a** and **1b**, respectively, and I_{1a1b} and I_{1b1a} are the cross-peak intensities.

$$k' = (1/t_m)\ln[(r+1)/(r-1)] \quad (5)$$

$$r = \{4X_{1a}X_{1b}(I_{1a1a}+I_{1b1b})/(I_{1a1b}+I_{1b1a})\} - (X_{1a}-X_{1b})^2 \quad (6)$$

Considering that the forward and reverse rates (R_1, R_{-1}) at the equilibrium **1a** ⇌ **1b** are equal (eq 7), the rate constants for the conversions **1a** → **1b** and **1b** → **1a** are given in eq 8.

$$R_1 = X_{1a}k_1 = X_{1b}k_{-1} = R_{-1} \quad (7)$$

$$k_1 = k'/(1+X_{1a}/X_{1b}) \text{ and } k_{-1} = k'/(1+X_{1b}/X_{1a}) \quad (8)$$

Two separate experiments were performed at each temperature. Within each experiment, two independent values of r_1 and r_2 were obtained from the intensities of C*H*= (**1a**)/CH_aH_b (**1b**) and CH_2 (**1a**)/CH_aH_b (**1b**) peaks, respectively. The averages of r_1 and r_2 from the two experiments r_{1-av} and r_{2-av} are listed in Table 2. The values of k'_{1-av} and k'_{2-av} were calculated from r_{1-av} and r_{2-av}, and their averages were used to yield k_1 and k_{-1}, which are the first-order rate constants for the conversions **1a** → **1b** and **1b** → **1a**, respectively. In the current systems, the exchange rates k_1 of 0.12(0.03) s^{-1} and k_{-1} of 0.035(0.008) s^{-1} at 297(1) K are much higher than those [$k_{for} = 10.71(0.10) \times 10^{-6}$ s^{-1} and $k_{rev} = 10.55(0.10) \times 10^{-5}$ s^{-1}, respectively, at 298(1) K] in the only other known, phosphine-promoted bis(alkylidene) ⇌ alkyl alkylidyne exchange $W(=CHSiMe_3)_2(CH_2SiMe_3)_2(PMe_3)$ ⇌ $W(\equiv CSiMe_3)(CH_2SiMe_3)_3(PMe_3)$.[7] k_1 and k_{-1} were then used in least-squares Eyring plots (Figure 2) to give the activation parameters.

The theoretical studies conducted by Prof. Zhen-Yang Lin and co-workers reveal that thermodynamically the d^0 alkylidyne complex $W(\equiv C\text{-}t\text{-}Bu)(CH_2\text{-}t\text{-}Bu)_2(Si\text{-}t\text{-}BuPh_2)$ (**1b**) and its bis(alkylidene) tautomer $W(=CH\text{-}t\text{-}Bu)_2(CH_2\text{-}t\text{-}Bu)(Si\text{-}t\text{-}BuPh_2)$ (**1a**) were close in energy, and the alkylidyne tautomer **1b** is slightly more stable.[18] These studies show that the relative stabilities of the tautomeric pairs of W and Mo alkylidyne complexes $M(\equiv CH)(CH_3)_2(X)$ and bis(alkylidene) complexes $M(=CH_2)_2(CH_3)(X)$ (X = Cl, CH_3, CF_3, SiH_3, and SiF_3) increase with the increasing π-accepting ability of X. When X is a silyl ligand, the tautomeric pair have similar stabilities. These results have been explained in terms of π interaction between ligand X and the electron density in the metal−alkylidyne/alkylidene bonds.

Reaction of a d^0 Silyl Alkylidyne Complex with O_2. Preparation and Characterization of a W Alkylidene Oxo Complex, W(=O)[=C(*t*-Bu)(Si-*t*-BuPh$_2$)](CH$_2$-*t*-Bu)$_2$ (2). When a yellow-orange solution of **1** in benzene-d_6 was exposed to 1 equiv of gaseous O_2 at room temperature, a rapid reaction occurred and the color of the solution turned red. We were surprised to find the formation of alkylidene oxo complex $W(=O)[=C(t\text{-}Bu)(Si\text{-}t\text{-}BuPh_2)](CH_2\text{-}t\text{-}Bu)_2$ (**2**) in this reaction in 32% yield by NMR (Scheme 2). Formally the silyl ligand

(14) Beck, S.; Lieber, S.; Schaper, F.; Geyer, A.; Brintzinger, H. *J. Am. Chem. Soc.* **2001**, *123*, 1483.
(15) Carpentier, J.; Maryin, V. P.; Luci, J.; Jordan, R. F. *J. Am. Chem. Soc.* **2001**, *123*, 898.
(16) Perrin, C. L.; Dwyer, T. J. *Chem. Rev.* **1990**, *90*, 935.
(17) Orrell, K. G.; Šik, V. *Annu. Rep. NMR Spectrosc.* **1993**, *27*, 103.
(18) Choi, S.-H.; Lin, Z.; Xue, Z. *Organometallics* **1999**, *18*, 5488.

Table 2. Exchange Rate Constants Derived from the 2D ^{1}H EXSY Spectra of 1a ⇌ 1b[b]

T[a] (K)	X_{1a}/X_{1b}	t_m (s)	r_{1-av}[b]	k'_{1-av}[c] (s^{-1})	r_{2-av}[b]	k'_{2-av}[c] (s^{-1})	k_1[d] (s^{-1})	k_{-1}[d] (s^{-1})
297	0.341(5)	0.3	4.832(3)	1.402(4)	4.578(4)	1.478(3)	1.10(4)	0.35(1)
292	0.307(6)	0.4	3.141(2)	0.832(2)	5.619(3)	0.901(4)	0.66(4)	0.20(1)
287	0.299(5)	0.5	9.772(3)	0.411(4)	8.547(4)	0.472(2)	0.34(3)	0.10(1)
282	0.289(4)	0.6	15.925(5)	0.213(2)	12.364(2)	0.269(3)	0.19(3)	0.054(8)
277	0.284(5)	0.7	22.053(4)	0.131(2)	15.925(5)	0.179(3)	0.12(3)	0.035(8)
272	0.276(2)	0.8	35.483(4)	0.071(4)	31.303(3)	0.079(2)	0.059(6)	0.016(1)
267	0.266(4)	1.0	55.054(6)	0.036(6)	42.667(8)	0.047(5)	0.033(6)	0.009(1)

[a] The estimated uncertainty in temperature measurement was 1 K. [b] r_1 and r_2 were calculated from the intensities of the C*H*═ (**1a**)/C*H*$_a$H$_b$ (**1b**) and C*H*$_2$ (**1a**)/CH$_a$*H*$_b$ (**1b**) peaks, respectively, according to eq 6. The averages r_{1-av} and r_{2-av} from two experiments are given here. [c] k'_{1-av} and k'_{2-av} were calculated from r_{1-av} and r_{2-av} according to eq 5. The total uncertainties $\sigma k/k$ in k'_1 and k'_2 were calculated from $\sigma k_{(ran)}/k$ and the estimated systematic uncertainty $\sigma k_{(sys)}/k = 5\%$ by $\sigma k/k = [(\sigma k_{(ran)}/k)^2 + (\sigma k_{(sys)}/k)^2]^{1/2}$. [d] k_1 and k_{-1} were calculated according to eq 8 from the averages of k'_{1-av} and k'_{2-av}.

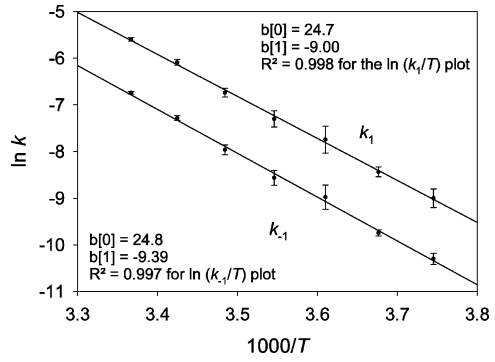

Figure 2. Eyring plots for the **1a** ⇌ **1b** exchange.

Scheme 2. Reactions of an Equilibrium Mixture 1a ⇌ 1b with O_2 and H_2O

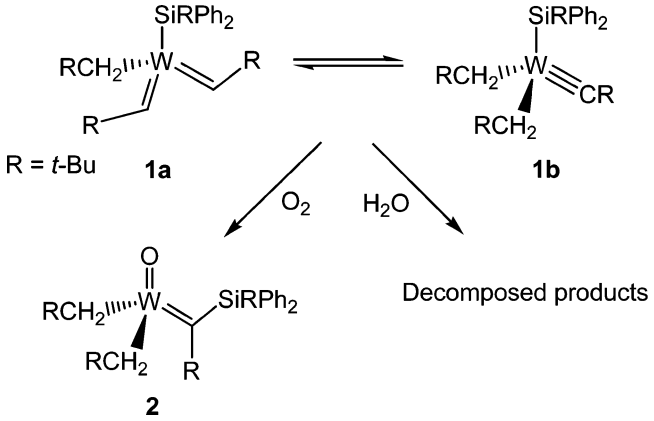

in W(≡C-*t*-Bu)(CH$_2$-*t*-Bu)$_2$(Si-*t*-BuPh$_2$) (**1b**) migrates to the alkylidyne ligand in this reaction to give the alkylidene ligand ═C(*t*-Bu)(Si-*t*-BuPh$_2$) in **2**. To our knowledge, this observation is the first such silyl ligand migration. Ahn and Mayr have reported a formal insertion of an alkylidyne group into a W−N bond and the elimination of HBr in the reaction of W(═CHPh)(═X)TpBr [Tp = tris(pyrazolyl)borate; X = NR, O] with Br$_2$.[19] The formation of **2** through the reaction of **1** with H_2O was excluded (Scheme 2).

Spectroscopic properties of **2** are consistent with the structure assignment. The alkylidene resonance of **2** at 269.65 ppm appears as a singlet in the ^{1}H-gated-decoupled ^{13}C NMR spectrum. The molecular structure of **2** has been determined by X-ray crystallography and is shown in Figure 3. Crystallographic data and selective bond lengths and angles are given in Tables 3 and 4.

(19) (a) Ahn, S.; Mayr, A. *J. Am. Chem. Soc.* **1996**, *118*, 7408. (b) Mayr, A.; Ahn, S. *Inorg. Chim. Acta* **2000**, *300*−*302*, 406.

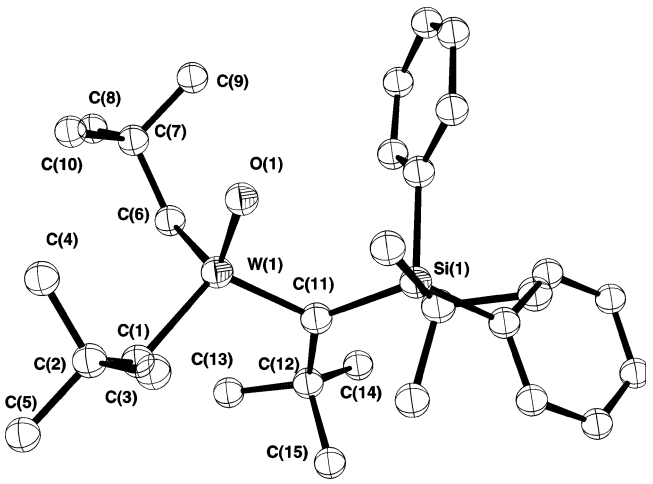

Figure 3. ORTEP of **2** showing 50% probability thermal ellipsoids.

Complex **2** exhibits distorted tetrahedral geometry around the W center with interligand angles in the range 104.1(3)−114.8(3)°. The W═C bond distance of 1.920(7) Å is similar to those observed in other d^0 tungsten alkylidene complexes.[20] The W═O bond distance of 1.686(5) Å is also similar to those observed in tungsten oxo complexes.[20a] **2**, which is thermally stable at room temperature, reacts further with excess O_2 to give unknown species.

Preparation and Characterization of W(≡C-*t*-Bu)(CH$_2$-*t*-Bu)$_2$(OSi-*t*-BuPh$_2$) (6) and Studies of the Mechanistic Pathway in the Formation of W(═O)[═C(*t*-Bu)(Si-*t*-BuPh$_2$)](CH$_2$-*t*-Bu)$_2$ (2). The interesting silyl migration reaction to give **2** likely proceeds through one of two possible pathways (Scheme 3). In pathway A, one O atom inserts into the W−Si bond in W(≡C-*t*-Bu)(CH$_2$-*t*-Bu)$_2$(Si-*t*-BuPh$_2$) (**1a**) to give the intermediate W(≡C-*t*-Bu)(CH$_2$-*t*-Bu)$_2$(OSi-*t*-BuPh$_2$) (**6**). This insertion is followed by −Si-*t*-BuPh$_2$ migration to the alkylidyne ligand to give **2**. In pathway B, −Si-*t*-BuPh$_2$ migration yields a d^2 W(IV) alkylidene complex **7** *prior* to silyl migration. The reaction of **7** with O_2 gives **8**, and then **2**.

To our knowledge, the silyl migration observed here and a silyl-substituted alkylidene oxo complex have not

(20) (a) Nugent, W. A.; Mayer, J. M. *Metal*−*Ligand Multiple Bonds*; Wiley: New York, 1988. (b) Churchill, M. R.; Youngs, W. J. *Inorg. Chem.* **1979**, *18*, 2454. (c) VanderLende, D. D.; Abboud, K. A.; Boncella, J. M. *Organometallics* **1994**, *13*, 3378. (d) Schrock, R. R.; DePue, R. T.; Feldman, J.; Yap, K. B.; Yang, D. C.; Davis, W. M.; Park, L.; DiMare, M.; Schofield, M.; Anhaus, J.; Walborsky, E.; Evitt, E.; Krüger, C.; Betz, P. *Organometallics* **1990**, *9*, 2262.

Table 3. Crystal Data and Structure Refinement for 2

empirical formula (fw)	$C_{31}H_{50}OSiW$ (650.65)
temperature	−50(2) °C
wavelength	0.71073 Å
cryst syst	orthorhombic
space group	$Pna2_1$
unit cell dimens	a = 21.8650(5) Å, α = 90° b = 17.2786(2) Å, β = 90° c = 8.31220(10) Å, γ = 90°
volume	3140.32(9) Å^3
Z	4
density(calcd)	1.376 Mg/m^2
abs coeff	3.736 mm^{-1}
F(000)	1328
cryst size	0.20 × 0.20 × 0.16 mm^3
θ range for data collection	1.50−28.26°
index ranges	$-28 \le h \le 28$, $-19 \le k \le 13$, $-11 \le l \le 4$
no. of reflns collected	9837
no. of indep reflns	3931 [R(int) = 0.0334]
completeness to θ = 23.32°	99.8%
abs corr	semiempirical from equivalents
refinement method	full-matrix least-squares on F^2
no. of data/restraints/params	3930/1/307
goodness-of-fit on F^2	1.035
final R indices [$I > 2\sigma(I)$][a]	R1 = 0.0291, wR2 = 0.0544
R indices (all data)[a]	R1 = 0.0529, wR2 = 0.0638
largest difference peak and hole	0.638 and −1.313 e·Å^{-3}
absolute struct param	0.015(13)

[a] wR2 = $[\sum w(F_o^2 - F_c^2)^2/\sum w(F_o^2)^2]^{1/2}$; $R = \sum||F_o| - |F_c||/\sum|F_o|$; $w = 1/[\sigma^2(F_o^2) + (aP)^2 + bP]$; $P = [2F_c^2 + \max(F_o^2,0)]/3$.

Table 4. Selected Bond Lengths (Å) and Angles (deg) for 2

W−O	1.686(5)	W−C(11)	1.920(7)
W−C(1)	2.112(9)	W−C(6)	2.118(9)
O−W−C(11)	104.1(3)	O−W−C(1)	111.8(3)
C(11)−W−C(1)	109.7(3)	O−W−C(6)	109.5(3)
C(11)−W−C(6)	109.0(3)	C(1)−W−C(6)	112.4(4)
C(11)−Si−C(26)	105.8(3)	C(11)−Si−C(20)	114.8(3)
C(26)−Si−C(20)	103.4(3)	C(11)−Si−C(16)	114.8(3)
C(2)−C(1)−W	125.6(5)	C(7)−C(6)−W	120.6(5)
C(9)−C(7)−C(8)	107.6(8)	C(9)−C(7)−C(10)	109.3(8)
C(8)−C(7)−C(10)	107.4(7)	C(9)−C(7)−C(6)	112.3(7)
C(12)−C(11)−Si	124.8(5)	C(12)−C(11)−W	114.4(5)
Si−C(11)−W	120.8(4)	C(18)−C(16)−Si	114.0(6)
C(17)−C(16)−Si	110.4(6)	C(21)−C(20)−Si	120.5(6)
C(19)−C(16)−Si	110.3(5)	C(25)−C(20)−Si	123.6(6)

been observed.[21] We have conducted studies to elucidate the mechanistic pathway in the formation of **2** in the current work. First we prepared W(≡C-*t*-Bu)(CH_2-*t*-Bu)$_2$(OSi-*t*-BuPh_2) (**6**), a proposed intermediate in pathway A, from the reaction of W(≡C-*t*-Bu)(CH_2-*t*-Bu)$_2$Cl (**4**) with LiOSi-*t*-BuPh_2 (**9**) to see if it converted to **2** (Scheme 4). **9** was prepared directly from Li-*t*-Bu and $(Ph_2SiO)_3$ in 73% yield.[22] NMR studies of **6** showed that it slowly decomposed in solution during crystallization at −30 °C. No isomerization from W(≡C-*t*-Bu)(CH_2-*t*-Bu)$_2$(OSi-*t*-BuPh_2) (**6**) to W(=O)[=C(*t*-Bu)(Si-*t*-BuPh_2)](CH_2-*t*-Bu)$_2$ (**2**) was however observed over a period of a week at room temperature. Pathway A to **2** in Scheme 3 is thus unlikely.

Scheme 3. Proposed Pathways in the Formation of 2

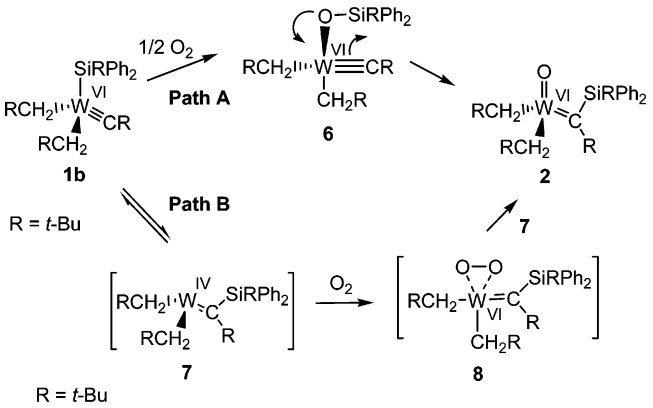

Scheme 4. Preparation of Silonate 9 and 6

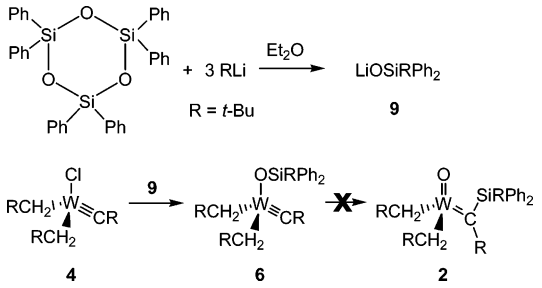

DFT Studies of the Mechanistic Pathway B. Theoretical studies have been conducted to explore the possibility of pathway B in the formation of **2**. All calculations were performed with the Gaussian 03 package[23] using the density functional theory method of B3LYP.[24] Full geometric optimizations were carried out with basis set I (BSI): LanL2DZ[25] for W with f polarization functions, for Si, Cl with d polarization functions,[26] and 6-311+G* for the rest of the elements. Single-point energies were calculated with basis set II (BSII): SDDAll for Si, Cl, and W, and 6-311++G** for other elements. Vibration frequency calculations were performed for all the structures with the BSI. The calculated relative energies shown in the text have been

(21) (a) Chisholm, M. H.; Hoffman, D. M.; Huffman, J. C. *Inorg. Chem.* **1983**, *22*, 4291. (b) Cotton, F. A.; Schwotzer, W.; Shamshoum, E. S. *Organometallics* **1984**, *3*, 1770. (c) Listemann, M. L.; Schrock, R. R. *Organometallics* **1985**, *4*, 74.

(22) MOSi-*t*-BuPh_2 (M = Li, **9**; Na, K) were initially prepared from silanol HOSi-*t*-BuPh_2 (Sieburth, S. M.; Mu, W. *J. Org. Chem.* **1993**, *58*, 7584) and alkali metals. The NMR spectra of these complexes showed that they were relatively pure compounds. However their reactions with **4** did not yield **6**. We suspect that the reactions between alkali metals and the silanol HOSiBu^tPh_2 perhaps were not complete.

(23) Frisch, M. J.; Trucks, G. W.; Schlegel, H. B.; Scuseria, G. E.; Robb, M. A.; Cheeseman, J. R.; Montgomery, J. A.; Vreven, Jr., T.; Kudin, K. N.; Burant, J. C.; Millam, J. M.; Iyengar, S. S.; Tomasi, J.; Barone, V.; Mennucci, B.; Cossi, M.; Scalmani, G.; Rega, N.; Petersson, G. A.; Nakatsuji, H.; Hada, M.; Ehara, M.; Toyota, K.; Fukuda, R.; Hasegawa, J.; Ishida, M.; Nakajima, T.; Honda, Y.; Kitao, O.; Nakai, H.; Klene, M.; Li, X.; Knox, J. E.; Hratchian, H. P.; Cross, J. B.; Adamo, C.; Jaramillo, J.; Gomperts, R.; Stratmann, R. E.; Yazyev, O.; Austin, A. J.; Cammi, R.; Pomelli, C.; Ochterski, J. W.; Ayala, P. Y.; Morokuma, K.; Voth, G. A.; Salvador, P.; Dannenberg, J. J.; Zakrzewski, V. G.; Dapprich, S.; Daniels, A. D.; Strain, M. C.; Farkas, O.; Malick, D. K.; Rabuck, A. D.; Raghavachari, K.; Foresman, J. B.; Ortiz, J. V.; Cui, Q.; Baboul, A. G.; Clifford, S.; Cioslowski, J.; Stefanov, B. B.; Liu, G.; Liashenko, A.; Piskorz, P.; Komaromi, I.; Martin, R. L.; Fox, D. J.; Keith, T.; Al-Laham, M. A.; Peng, C. Y.; Nanayakkara, A.; Challacombe, M.; Gill, P. M. W.; Johnson, B.; Chen, W.; Wong, M. W.; Gonzalez, C.; Pople, J. A. *Gaussian 03*, Revision B.03; Gaussian, Inc.: Pittsburgh, PA, 2003.

(24) (a) Becke, A. D. *Phys. Rev.* **1988**, *A38*, 3098. (b) Becke, A. D. *J. Chem. Phys.* **1993**, *98*, 1372, 5648. (c) Lee, C.; Yang, W.; Parr, R. G. *Phys. Rev.* **1988**, *B37*, 785.

(25) (a) Huzinaga, S. Andzelm, J.; Klobukowski, M.; Radzio-Andzelm, E.; Sakai, Y.; Tatewaki, H. *Gaussian Basis Sets for Molecular Calculations*; Elsevier: Amsterdam, 1984. (b) Wadt, W. R.; Hay, P. J. *J. Chem. Phys*. **1985**, 82, 284.

Scheme 5. Different Migration Groups R in the Equilibrium of 11a−f ⇌ 12a−f

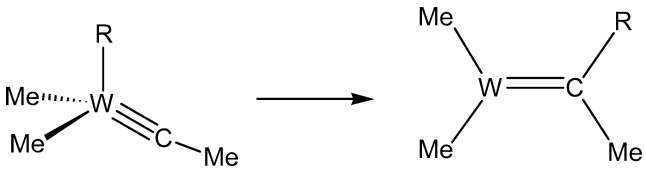

corrected with zero-point energy (ZPE). Atomic charges were analyzed by natural bond analysis.[27]

Theoretical Studies of the Silyl Migration. As depicted in Scheme 3, the key step in pathway B is the 1,2-silyl migration from W to the alkylidyne C atom. Therefore, we first studied a series of 1,2-migration reactions[28] with different migrating groups including H, CH_3, Cl, and three silyl groups (Scheme 5) to have a good understanding of the general features of the reaction. Among them, the $-SiMe_3$ ligand in **11e** is to model the $-Si$-*t*-$BuPh_2$ ligand in W(≡C-*t*-Bu)(CH_2-*t*-$Bu)_2$(Si-*t*-$BuPh_2$) (**1b**), while $-Si(SiH_3)_3$ in **11f** acts as a model for the $-Si(SiMe_3)_3$ ligand in W(≡C-*t*-Bu)(CH_2-*t*-$Bu)_2$[$Si(SiMe_3)_3$] (**3**). The migration reaction can be formally regarded as a reductive elimination that reduces W(VI) in the silyl alkylidyne complexes to W(IV). The W(IV)-alkylidene intermediates are a d^2 system. Therefore, they can be in either low-spin state ($S = 0$, singlet) or high-spin state ($S = 1$, triplet). Calculated structures of W-alkylidyne reactant **11e** and W-alkylidene intermediate in singlet state **12e(S)** and triplet state **12e(T)**, derived from the silyl migration of **11e**, are shown in Figure 4. **11e** adopts a distorted tetrahedral geometry with a small Si−W≡C angle of 93°. Although in different spin states, **12e(S)** and **12e-(T)** have quite similar geometries; both are in a planar geometry like the organic double bond. The high-spin species has a slightly longer W=C bond. All intermediates derived from other compounds have planar geometries.[13]

Since no perpendicular isomer was located, the planar geometry of **12** reveals that the W=C π bond is formed by the d_{yz} of W and the p_z of the C atoms. The π antibonding character makes d_{yz} the highest d orbital (Scheme 6). In the meanwhile, the recombined $d_{x^2-y^2}$ and d_{xy} orbitals are destabilized by the ligands in the *xy* plane, while d_{z^2} and d_{xz} remain basically unchanged. Although not totally degenerated, the energy levels of d_{xz} and d_{z^2} are very close. Therefore, the two d electrons in W(IV) prefer to occupy both d_{xz} and d_{z^2}, giving a high-spin state (Scheme 6). As shown in Table 5, for each migrating ligand, the reaction is endothermic. For each system, the high-spin state is ca. 36−40 kJ/mol more stable than the low-spin state in the migration product **12**. Therefore, further reactions were studied only with the high-spin state products.

It is interesting that the reaction energy for the migration reaction varies significantly with different

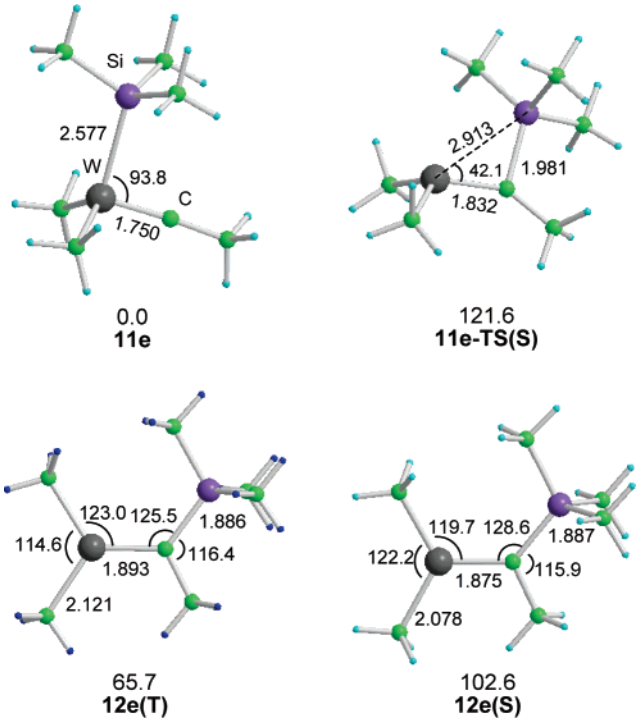

Figure 4. Calculated geometries and relative energies of **11e**, the singlet transition state **11e-TS(S)**, and the triplet and singlet products of silyl migration in **11e** (bond length: Å; bond angle: deg; energy: kJ/mol).

Scheme 6

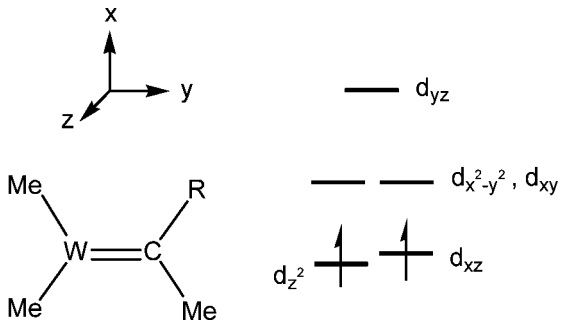

Table 5. Calculated Reaction Energies (kJ/mol) with ZPE Corrections of Migration Reactions of 11a−f

	reactant	Δ*E* (high spin)	Δ*E* (low spin)
R = H (**11a**)	0.0	65.1	102.1
R = CH_3 (**11b**)	0.0	96.4	133.0
R = Cl (**11c**)	0.0	258.7	298.8
R = SiH_3 (**11d**)	0.0	78.1	115.1
R = $SiMe_3$ (**11e**)	0.0	65.7	102.6
R = $Si(SiH_3)_3$ (**11f**)	0.0	112.2	151.9

ligands. Migrations of the H atom in **11a** and a methyl group in **11b** cost ca. 65.1 and 96.4 kJ/mol, respectively. However, the Cl migration in **11e** is very difficult, having a reaction energy of ca. 258.7 kJ/mol. Among the four silyl groups, $-SiMe_3$ has the lowest reaction energy (65.7 kJ/mol), while $-Si(SiH_3)_3$ has the highest reaction energy (112.2 kJ/mol). The 46.5 kJ/mol difference in the reaction energy between **11e** and **11f** is consistent with the observation that only W(≡C-*t*-Bu)(CH_2-*t*-$Bu)_2$(Si-*t*-$BuPh_2$) (**1b**), with a $-Si$-*t*-$BuPh_2$ ligand, undergoes the migration/oxidation reaction to give the W oxo complex **2**, while W(≡C-*t*-Bu)(CH_2-*t*-$Bu)_2$[$Si(SiMe_3)_3$] (**3**), with a $-Si(SiMe_3)_3$ ligand, does not.

(26) (a) Ehlers, A. W.; Böhme, M.; Dapprich, S.; Gobbi, A.; Höllwarth, A.; Jonas, V.; Köhler, K. F.; Stegmann, R.; Veldkamp, A.; Frenking, G. *Chem. Phys. Lett.* **1993**, *208*, 111. (b) Höllwarth, A.; Böhme, M.; Dapprich, S.; Ehlers, A. W.; Gobbi, A.; Jonas, V.; Köhler, K. F.; Stegmann, R.; Veldkamp, A.; Frenking, G. *Chem. Phys. Lett.* **1993**, *208*, 237.

(27) Reed, A. E.; Curtiss, L. A.; Weinhold, F. *Chem. Rev.* **1988**, *88*, 899.

(28) Suresh, C. H.; Koga, N. *Organometallics* **2001**, *20*, 4333.

Table 6. Calculated Structural Parameters, Natural Charges, and Wiberg Bond Indices of W Alkylidyne Complexes (bond lengths: Å; bond angles: deg)

					natural charge			Wiberg bond index	
	W≡C	W−R	W−C	R−W≡C	q^W	$q^{X\,a}$	q^R	W≡C	W−X
R = H **(11a)**	1.745	1.726	2.100	97.3	0.94	-0.20	-0.20	2.635	0.886
R = CH_3 **(11b)**	1.748	2.112	2.112	103.0	1.06	-0.95	-0.31	2.610	0.880
R = Cl **(11c)**	1.744	2.303	2.101	108.2	0.97	-0.32	-0.32	2.541	0.907
R = SiH_3 **(11d)**	1.748	2.569	2.098	92.5	0.76	0.38	-0.12	2.596	0.894
R = $SiMe_3$ **(11e)**	1.750	2.577	2.103	93.8	0.74	1.28	0.01	2.596	0.858
R = $Si(SiH_3)_3$ **(11f)**	1.750	2.565	2.099	95.5	0.81	-0.38	-0.19	2.581	0.865

[a] X is the atom of group R that directly connects to W.

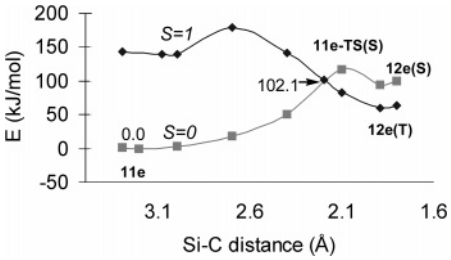

Figure 5. Schematic representation of the singlet and triplet PES along the Si−C distance in the silyl migration process.

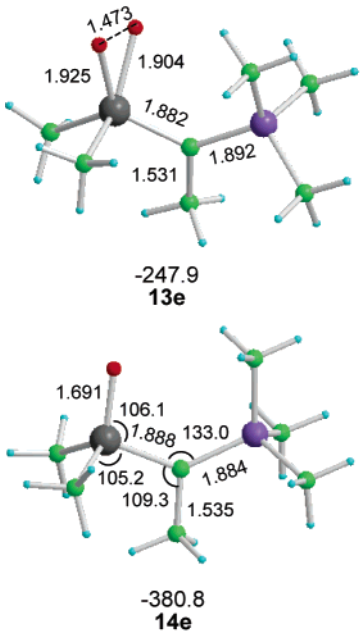

Figure 6. Calculated geometries and relative energies of O_2 adduct (**13e**) of **12e** for the reaction of **11e** with O_2 and the final oxidation product of **14e** (bond length: Å; bond angle: deg; energy: kJ/mol).

The reaction energies are roughly correlated with the calculated R−W≡C angles and the bond strength in the reactant, as shown in Table 6. Chlorine is a good π-donor to the empty d orbitals of the metal center, and the donation strengthens the W−Cl bond in **11c**. The lone pair on the chlorine atom are also repulsive with the π orbitals of the W≡C bond in **11c**. As a result, the Cl−W≡C angle (108.2°) in **11c** is the largest. On the other hand, the silyl ligands in **11d**−**f** are π-acceptors. However, they cannot receive back-donation from the d^0 W(VI) centers to strengthen the W−Si bonds, but can have stabilizing interaction with the in-plane π orbital of the W≡C bonds. Therefore, the Si−W≡C angles are small, close to 90°. The three methyl groups in $-SiMe_3$ in **11e** behave as electron-withdrawing groups,[29] while the three $-SiH_3$ groups in $Si(SiH_3)_3$ in **11f** are electron-donating groups. As a result, the former has a smaller Si−W≡C angle than the latter. This is also indicated by the calculated NBO charges, as shown in Table 6. Among the three compounds **11d**−**f** with a silyl group, the electron density of the Si−W bond gradually shifts from the Si to W in the order $Si(SiH_3)_3$, SiH_3, and $SiMe_3$. **11e** has a less positive W and a slightly positive silyl group. On the other hand, **11f** has a more positive W and a negative silyl group. This order parallels with the calculated relative reaction energies. It seems that the electron-poor silyl ligand facilitates such a migration reaction, because low electron density on the Si will increase its π-accepting ability, which promotes the tautomerization of a W alkylidyne to a W bis(alkylidene) complex.[18]

We have located the transition state [**11e-TS(S)**] for the formation of silyl migration product from **11e** in low-spin configuration (Figure 5). The calculated activation energy is ca. 121.6 kJ/mol, and ca. 19.0 kJ/mol higher than the reaction energy. As depicted in Figures 4 and 5, **11e-TS(S)** closely resembles the product **11e**(**S**), indicating a late transition state. The transition state could not be located in high-spin configuration. Since the silyl migration reaction is product determined (endothermic) and the high-spin state is ca. 36−40 kJ/mol more stable than the low-spin state, according to the Hammond postulate the real transition state is expected to be more stable than the low-spin transition state **11e-TS**(**S**). While the location of a true transition state for the silyl migration is difficult because it involves a spin-crossing, we approximated the transition state by locating the crossing point of the potential surfaces of the two states. The partial optimization approach was adopted to locate the two-state crossing point.[30] The Si−C bond was chosen as the reaction coordinate. A set of Si−C bond-fixed structures were separately optimized at two different potential energy surfaces ($S = 0$ and $S = 1$). The result is shown in Figure 5. The crossing point of the two states occurs earlier than the low-spin transition state **11e-TS(S)**. That means the system switches from a low-spin state to the high-spin state without passing the low-spin transition state. A barrier of about 102.1 kJ/mol was found with the crossing point.

(29) Carbon is more electronegative than silicon (the Pauling electronegativities of carbon and silicon are 2.55 and 1.90, respectively).

(30) (a) Harvey, J. N. In *Computational Organometallic Chemistry*, Cundari, T. R., Ed.; Marcel Dekker: New York, 2001. (b) Poli, R.; Harvey, J. N. *Chem. Soc. Rev.* **2003**, *32*, 1.

Theoretical Studies of the O_2 Attack. The reaction between **11e** and dioxygen was then studied. First of all, we found that **11e** cannot form a stable complex with O_2. That is in line with the assumption that the oxidation takes place after silyl migration. Since the silyl migration step is endothermic, it is expected that the O_2 attack assists the shifting of the equilibrium **11e** ⇌ **12e** toward **12e**. The intermediate **12(T)** reacts with O_2, leading to three possible spin states, $S = 0$, $S = 1$, or $S = 2$, depending upon the ways of coupling the spins on the W atom with the spin on O_2. However, all efforts to locate the $S = 1$ and $S = 2$ intermediates failed. Only the singlet intermediate **13e** with an energy of −247.9 kJ/mol with respect to separated **11e** and O_2 was found. In intermediate **13e**, the O_2 occupies one of the tetrahedral positions. It is nearly coplanar with one of the W−CH_3 bonds. The two W−O bonds are 1.925 and 1.904 Å, respectively. The O−O distance is about 1.473 Å, indicating that it is a typical peroxo O−O bond. The O_2 binding process is considered to undergo a three-center oxidative addition. The reaction is exothermic by about −313.6 kJ/mol. No transition state could be located for this coupling reaction between the two diradical species.

The conversion of **13e** to the final product **14e** (a model of **2**) might occur with different pathways because **13e** should be a very reactive species. One possibility is that **13e** reacts with **12e(T)** to give two molecules of **14e**. We have not calculated a transition state for the reaction. However, the calculated large exothermicity of ca. −380.8 kJ/mol for the reaction suggests that the oxygen transfer from peroxo complex **13e** to **12e(T)** should be a very fast process. We suggest that it is this remarkably high exothermic driving force that pushes the whole reaction. In other words, this is an oxygen-induced silyl migration.

The theoretical calculations here on model 1,2-migrations from W(Me)$_2$(R)(≡CH) to W(Me)$_2$(=CHR) indicate that the reactivity is sensitive to the nature of the −R ligand. −$SiMe_3$ migration is much more favorable than −Si($SiMe_3$)$_3$ migration. The results suggest that the formation of **2** from the reaction of **1b** with O_2 might be initiated by a 1,2-silyl migration in **1b** to generate a triplet W(IV)-alkyldene intermediate, which is trapped by O_2.

Experimental Section

General Procedures. All manipulations, unless otherwise noted, were performed under a dry nitrogen atmosphere with the use of either a drybox or standard Schlenk techniques. All solvents were purified by distillation from potassium/benzophenone ketyl. Benzene-d_6 and toluene-d_8 were dried over activated molecular sieves and stored under N_2. One-dimensional ^{1}H and ^{13}C NMR spectra, unless noted, were recorded at 23 °C on a Bruker AC-250 or AMX-400 Fourier transform (FT) spectrometer and referenced to solvents (residual protons in the ^{1}H spectra). ^{1}H−^{13}C heteronuclear correlation (HETCOR) and ^{29}Si{^{1}H} (DEPT) NMR experiments were conducted at 23 °C on a Bruker AMX-400 FT spectrometer. The ^{29}Si{^{1}H} (DEPT) NMR spectra were referenced to $SiMe_4$. 2D NOESY spectra were recorded at 23 °C on a Varian Mercury 300 FT spectrometer (ns = 32, t_{mix} = 3 s, increments = 128). 2D EXSY spectra (297−267 K) were recorded on an updated Bruker AMX-400 FT spectrometer. Li(THF)$_3$Si-*t*-$BuPh_2$ (**5**)[12] and W(≡C-*t*-Bu)(CH_2-*t*-Bu)$_3$[12] were prepared by the literature procedures. HCl in Et_2O (1.0 M, Aldrich) was used as received. O_2 gas (99.6% purity) was dried by passing through a −78 °C trap and was transferred quantitatively through a gas manifold. Li-*t*-Bu in pentane (Strem, 2.0 M) was purified by removing pentane in vacuo and subliming the residue at 50−60 °C to give Li-*t*-Bu as a solid on a coldfinger. Elemental analyses were performed by Complete Analysis Laboratories Inc., E&R Microanalytical Division, Parsippany, NJ 07054-4909.

Preparation of 1 [W(=CH-*t*-Bu)$_2$(CH_2-*t*-Bu)(Si-*t*-$BuPh_2$) (1a) ⇌ W(≡C-*t*-Bu)(CH_2-*t*-Bu)$_2$(Si-*t*-$BuPh_2$) (1b)]. HCl (0.54 mmol, 1.0 M in Et_2O) was added dropwise to a vigorously stirred solution of W(≡C-*t*-Bu)(CH_2-*t*-Bu)$_3$ (0.25 g, 0.54 mmol) in Et_2O (30 mL) at −78 °C. The color of the solution changed slowly from dark yellow to green-yellow when the solution was allowed to gradually warm to −40 °C in 3 h. All the volatiles were removed under vacuum at −40 °C. Li(THF)$_3$Si-*t*-$BuPh_2$ (**5**, 0.25 g, 0.54 mmol) in Et_2O was added dropwise to the solid at −40 °C, and the solution was warmed slowly to −10 °C. Removal of volatiles in vacuo, followed by extraction with pentane, filtration, and crystallization at −30 °C gave 0.20 g of **1** (0.32 mmol, 58% yield). Data for **1**: Anal. Calcd for $C_{31}H_{50}SiW$: C, 58.67; H, 7.94. Found: C, 58.30; H, 8.31. Data for **1a**: ^{1}H NMR (benzene-d_6, 250.1 MHz) δ 7.79−7.75, 7.24−7.15 (m, 10H, C_6H_5), 2.08 (d, 2H, $CH_aH_bCMe_3$, $^2J_{H-H}$ = 11.9 Hz), 1.53 (s, 9H, ≡CCMe_3), 1.28 (s, 9H, SiCMe_3Ph_2), 1.06 (s, 18H, CH_2CMe_3), −0.77 (d, 2H, $CH_aH_bCMe_3$); ^{13}C{^{1}H} (benzene-d_6, 62.9 MHz) δ 318.38 (≡CCMe$_3$), 143.81, 137.90, 128.59, 127.91 (C_6H_5), 134.52 (CH_2CMe_3), 53.87 (≡CCMe$_3$), 37.66 (CH_2CMe_3), 34.14 (CH_2CMe_3), 32.29 (≡CCMe_3), 30.60 (SiCMe$_3$), 21.63 (SiCMe_3); ^{29}Si{^{1}H} NMR (benzene-d_6, 79.5 MHz) δ 73.74 (*Si*-*t*-$BuPh_2$). Data for **1b**: ^{1}H NMR (benzene-d_6, 250.1 MHz) δ 7.86−7.84, 7.24−7.15 (m, 10H, C_6H_5), 6.03 (s, 2H, =CHCMe$_3$), 1.29 (s, 9H, SiCMe_3Ph_2), 1.19 (s, 18H, =CHCMe_3), 0.96 (s, 9H, CH_2CMe_3), 0.35 (s, 2H, CH_2CMe_3); ^{13}C{^{1}H} (benzene-d_6, 62.9 MHz) δ 272.32 (=CHCMe$_3$, $^1J_{C-H}$ = 104.1 Hz), 144.31, 137.69, 128.18, 127.61 (C_6H_5), 131.21 (CH_2CMe_3), 45.49 (=CHCMe$_3$), 37.31 (CH_2CMe_3), 35.01 (CH_2CMe_3), 32.04 (=CHCMe_3), 30.30 (SiCMe_3), 20.69 (SiCMe_3); ^{29}Si{^{1}H} NMR (benzene-d_6, 79.5 MHz) δ 62.11 (*Si*-*t*-$BuPh_2$).

Preparation of W(=O)[=C(*t*-Bu)(Si-*t*-$BuPh_2$)](CH_2-*t*-Bu)$_2$ (2). 1 (0.50 g, 0.79 mmol) was dissolved in 2.0 mL of benzene-d_6 in a J. Young NMR tube, and the solution was frozen at −60 °C. The tube was then evacuated, and O_2 (0.79 mmol) was introduced into the NMR tube. The solution was then warmed to room temperature. In 20 min, the color of the solution changed from brown to red-orange. All the volatiles were then removed in vacuo. NMR spectra of the solid showed that ca. 32% (0.25 mmol) of **2** had reacted with O_2; 68% of **1** still remained in the reaction mixture. The solid was redissolved in pentane, and the solution was filtered. Slow cooling of the solution to −30 °C gave **2** as a crystalline solid (isolated weight: 8.8 mg, 0.014 mmol, 5.5% yield based on the amount of **1** that had reacted with O_2). Data For **2**: ^{1}H NMR (benzene-d_6, 250.1 MHz) δ 7.79, 7.22−7.15 (m, 10H, Si-*t*-BuPh_2), 3.27 (d, 2H, $CH_aH_bCMe_3$, $^2J_{H-H}$ = 14.1 Hz), 1.31 (s, 9H, SiCMe_3-Ph_2), 1.52 [s, 9H, =C(SiCMe$_3$Ph$_2$)CMe_3], 1.19 (s, 18H, $CH_aH_bCMe_3$), 0.34 (d, 2H, $CH_aH_bCMe_3$); ^{13}C{^{1}H} (benzene-d_6, 62.9 MHz) δ 269.65 (W=C), 138.56, 136.52, 130.68, 127.81 (Si-*t*-BuPh_2), 130.06 (CH_2CMe_3), 48.24 [=C(SiCMe$_3$Ph$_2$)CMe$_3$], 36.08 (CH_2CMe_3), 35.27 (CH_2CMe_3), 34.53 [=C(SiCMe$_3$Ph$_2$)CMe_3], 31.48 (SiCMe_3), 23.56 (SiCMe_3). Anal. Calcd for $C_{31}H_{50}OSiW$: C, 57.22; H, 7.75. Found: C, 56.93; H, 7.88.

Preparation of LiOSi-*t*-$BuPh_2$ (9). To a solution of hexaphenylcyclotrisiloxane (1.428 g, 2.40 mmol, Gelest) in Et_2O (30 mL) at −56 °C with stirring was added dropwise Li-*t*-Bu (0.554 g, 8.64 mmol) in pentane (40 mL) at −56 °C. The mixture was stirred and gradually warmed to 23 °C overnight. The solution was then refluxed at 40 °C overnight. All the volatiles were then removed in vacuo to give **9** as a crude white solid (1.38 g, 5.26 mmol, 73% yield). The solid was then washed with cold hexanes and subsequently dried before being submitted for elemental analysis. Data For **9**: ^{1}H NMR (benzene-

d_6, 250.1 MHz) δ 7.71−7.55, 7.22−7.15 (m, 10H, C_6H_5), 0.97 (s, 9H, CMe_3); $^{13}C\{^1H\}$ (benzene-d_6, 62.9 MHz) δ 134.80, 129.08, 127.06, 126.67 (C_6H_5), 28.43 (CMe_3), 27.21 (CMe$_3$). Anal. Calcd for $C_{16}H_{19}OSiLi$: C, 73.25; H, 7.30. Found: C, 73.18; H, 7.29.

Preparation of W(≡C-*t*-Bu)(CH$_2$-*t*-Bu)$_2$(OSi-*t*-BuPh$_2$) (6). Anhydrous HCl (0.32 mmol, 1.0 M in Et_2O) was added dropwise with vigorous stirring over a 30 min period to W(≡C-*t*-Bu)(CH$_2$-*t*-Bu)$_3$ (0.146 g, 0.313 mmol) in Et_2O (10 mL) at −78 °C. The solution was warmed to 0 °C over a period of 2 h and then stirred for 20 min. A solution of LiOSi-*t*-BuPh$_2$ (**9**) (0.082 g, 0.313 mmol) in Et_2O (10 mL) was added at −30 °C. The mixture was warmed to room temperature in 40 min and then stirred for another 20 min. The volatiles were removed in vacuo, and the residue was dissolved in a small amount of hexanes and filtrated. Volatiles in the filtrate were removed to give a dark red oil. 4,4′-Dimethylbiphenyl (5.0 mg) as an NMR internal standard was added, and the ^1H NMR of the mixture showed the yield of **6** at 32%. **6** was found unstable, and repeated attempts to purify it by crystallization led to the formation of dark red crystals of **6** mixed with unknown solid impurities.

In another preparation of **6** involving 0.227 g (0.487 mmol) of W(≡C-*t*-Bu)(CH$_2$-*t*-Bu)$_3$, 0.487 mL (0.487 mmol) of 1.0 M HCl in Et_2O, and 0.128 g (0.487 mmol) of LiOSi-*t*-BuPh$_2$ (**9**) by a similar procedure, 4.0 mg of dark red crystals for elemental analysis reported below were isolated from the solid precipitation from a pentane solution at −30 °C.

Data For **6**: ^1H NMR (benzene-d_6, 250.1 MHz) δ 7.79−7.19 (m, 10H, C_6H_5), 1.88 (d, 2H, CH_aH$_b$CMe$_3$, $^2J_{H-H}$ = 14.4 Hz), 1.36 (d, 2H, CH$_a$$H_bCMe_3$), 1.22 (s, 18H, CH$_aH_bCMe_3$), 1.20 (s, 9H, ≡CC$Me_3$), 1.18 (s, 9H, SiC$Me_3$); $^{13}C\{^1H\}$ (benzene-d_6, 62.9 MHz) δ 314.13 (W≡CCMe$_3$), 135.44−127.84 (C_6H_5), 97.06 (CH$_2$-CMe$_3$), 52.01 (≡CCMe$_3$), 34.37 (CH$_2$CMe_3), 33.94 (CH$_2$$CMe_3$), 32.71 (≡CC$Me_3$), 27.12 (SiC$Me_3$), 20.18 (Si$CMe_3$). Anal. Calcd for $C_{31}H_{50}OSiW$: C, 57.22; H, 7.75. Found: C, 57.22; H, 8.06.

Reaction of W(≡C-*t*-Bu)(CH$_2$-*t*-Bu)$_2$[Si(SiMe$_3$)$_3$] (3) with O$_2$. **3** (43.9 mg, 0.0683 mmol) in benzene-d_6 was added to 1.5 equiv of O_2 in a J. Young NMR tube. The mixture was kept at 23 °C for 6 h. A ^1H NMR spectrum of the solution then revealed that HSi(SiMe$_3$)$_3$ was the major product along with other unidentified compounds.

Thermodynamic Studies of the 1a ⇌ 1b Exchange. For the thermodynamic studies, the equilibrium constants K_{eq} were obtained from at least two separate experiments at a given temperature, and their averages are listed (Table 1). The *maximum* random uncertainty in the equilibrium constants was combined with the estimated systematic uncertainty, ca. 5%. The total uncertainties in the equilibrium constants were used in the ln K_{eq} vs 1/T plot in Figure 1 and error propagation calculations. The estimated uncertainty in the temperature measurements for an NMR probe was 1 K. The enthalpy ($\Delta H°$) and entropy ($\Delta S°$) changes were calculated from an unweighted nonlinear least-squares procedure contained in the SigmaPlot Scientific Graph System. The uncertainties in $\Delta H°$ and $\Delta S°$ were computed from the following error propagation formulas (eqs 9 and 10), which were derived from $-RT \ln K_{eq} = \Delta H° - T\Delta S°$.

$$(\sigma\Delta H°)^2 = (\sigma T/T)^2R^2(T_{max}^2T_{min}^4 + T_{min}^2T_{max}^4) \times [\ln(K_{eq(max)}/K_{eq(min)})]^2/\Delta T^4 + 2R^2T_{max}^2T_{min}^2(\sigma K_{eq}/K_{eq})^2/\Delta T^2 \quad (9)$$

$$(\sigma\Delta S°)^2 = 2R^2T_{min}^2T_{max}^2[\ln(K_{eq(max)}/K_{eq(min)})]^2 \times (\sigma T/T)^2/\Delta T^4 + R^2(T_{max}^2 + T_{min}^2)(\sigma K_{eq}/K_{eq})^2/\Delta T^2 \quad (10)$$

where $\Delta T = (T_{max} - T_{min})$.[8]

Kinetic Studies of the 1a ⇌ 1b Exchange. In the kinetic studies by 2D EXSY, the pulse sequence was t_0−90°−t_1−90°−t_m−90°−FID. The initial relaxation delay time t_0 was typically 3 s (>4T_1, vide infra), the initial t_1 was 3 μs, and the mixing time t_m was varied according to the experimental temperature (vide infra). The pulse sequence was repeated for 128 values of t_1; that is, the F_1 dimension contained 128 points. The number of scans per experiment was 32, giving a total experiment time of ~270 min. The optimal mixing time $t_{m,opt}$ was chosen on the basis of eq 11 to minimize the relative error in the rate constant.[15] The activation parameters determined from the Eyring analysis (Figure 2) were obtained by using the average rate constants k_1 and k_{-1} for the temperature range from 267 to 297 K. The activation enthalpies ($\Delta H^‡$) and entropies ($\Delta S^‡$) were calculated from an unweighted nonlinear least-squares procedure contained in the SigmaPlot Scientific Graph System. Spin−lattice relaxation times T_1 were measured by using the standard inversion−recovery method. T_1 values for the hydrogen atoms of **1a** and **1b** measured at 287 and 267 K are listed in Table 7.

Table 7. T_1 (s) Values for the α-H Atoms of 1a and 1b at 287 and 267 K

T (K)	CH= (**1a**)	CH_2 (**1a**)	C$H_a$$H_b$ (**1b**)	C$H_a$$H_b$ (**1b**)
287	1.35	0.86	0.67	0.63
267	1.19	0.55	0.33	0.33

$$t_{m,opt} \approx 1/(T_1^{-1} + k_1 + k_{-1}) \quad (11)$$

Control experiments established that rate constants determined by EXSY are not significantly affected by a ±50% variation in $t_{m,opt}$. Uncertainties in rate constant values were estimated assuming ±1% uncertainty in the finite *s*/*N* ratios of the computed spectra and ±2% uncertainty in 2D signal integrations. At least two separate experiments performed for all temperatures gave the uncertainty. The *maximum* random uncertainty in the equilibrium constants was combined with the estimated systematic uncertainty, ca. 5%. The total uncertainties in the rate constants were used in the Eyring plots in Figure 2 and error propagation calculations. The estimated uncertainty in the temperature measurements for an NMR probe was 1 K. The uncertainties in $\Delta H^‡$ and $\Delta S^‡$ were computed from the following error propagation formulas (eqs 12 and 13), which were derived from $R \ln(kh/k_bT) = -\Delta H^‡/T + \Delta S^‡$.[31]

$$(\sigma\Delta H^‡)^2 = R^2T_{max}^2T_{min}^2/\Delta T^2\{(\sigma T/T)^2[(1 + T_{min}\Delta L/\Delta T)^2 + (1 + T_{max}\Delta L/\Delta T)^2] + 2(\sigma k/k)^2\} \quad (12)$$

$$(\sigma\Delta S^‡)^2 = R^2/\Delta T^2\{(\sigma T/T)^2[T_{max}^2(1 + T_{min}\Delta L/\Delta T)^2 + T_{min}^2(1 + T_{max}\Delta L/\Delta T)^2] + (\sigma k/k)^2(T_{max}^2 + T_{min}^2)\} \quad (13)$$

where $\Delta L = [\ln(k_{max}/T_{max}) - \ln(k_{min}/T_{min})]$ and $\Delta T = (T_{max} - T_{min})$.

X-ray Crystal Structure Determination for 2. The structure of **2** was determined at the University of Delaware. A suitable crystal was selected and mounted in a thin-walled glass capillary under an inert atmosphere. The data were collected on a Siemens P4 diffractometer equipped with a SMART/CCD detector. The systematic absences in the diffraction data are consistent for space groups $Pna2_1$ and $Pnma$. Even though the E-statistics suggested the centrosymmetric space group, the value of Z and the absence of a molecular mirror plane indicated the non-centrosymmetric space group. Both possibilities were explored, but the only solution in the non-centrosymmetric option yielded chemically reasonable and computationally stable results of refinement. The structure of **2** was solved using direct methods, completed by subsequent

(31) More, P. M.; Spencer, M. D.; Wilson, S. R.; Girolami, G. S. *Organometallics* **1994**, *13*, 1646.

difference Fourier syntheses, and refined by full-matrix least-squares procedures. Absorption corrections were not required because there was less than 10% variation in the integrated ψ-scan intensity data. All non-hydrogen atoms were refined with anisotropic displacement coefficients, and hydrogen atoms were treated as idealized contributions. All software and sources of the scattering factors are contained in the SHELXTL (5.03) program library (G. Sheldrick, Siemens XRD, Madison, WI).

Acknowledgment is made to the National Science Foundation (CHE-9457368, CHE-9904338, and CHE-0212137) and the Research Grant Council of Hong Kong (HKUST6193/00P) for financial support.

Supporting Information Available: Partial solid-state CPMAS $^{13}C\{^1H\}$ and 2D EXSY NMR spectra of the **1a** ⇌ **1b** exchange, a complete list of crystallographic data for **2**, calculated total energies and calculated geometries with coordinates of **11a**−**14e**. These materials are available free of charge via the Internet at http://pubs.acs.org.

OM049031J